糖尿病

加齢とともに耐糖能は低下し、糖尿病の頻度は増加する。インスリン分泌や身体活動量の低下、体組成の変化（筋肉組織量の低下、脂肪組織量の増加）、ミトコンドリア機能障害などによるインスリン抵抗性の増加などがその原因として挙げられる。

高血糖は高齢者においても糖尿病細小血管症および大血管症の危険因子であり、血糖の正常化に努めるべきである。

また特に後期高齢者では糖尿病に合併した、認知症、鬱などが生活機能を低下させるため、高齢者総合機能評価（CGA）を用いたアプローチが必要となる。

① 診断

高齢者でも糖尿病の診断は若年者と同様の基準を用いる。高齢者では空腹時血糖値と比較し糖負荷後血糖値が上昇する頻度が高くなるため、空腹時血糖値で糖尿病と診断されなくても、糖負荷後高血糖から診断されることが多い。糖負荷後高血糖は、若年者では大血管症および細小血管症の危険因子であることが明らかにされつつあるが、高齢者でも冠動脈死、あるいは全死亡の重要な危険因子とされる。即ち、高齢者糖尿病の診断では、糖負荷後高血糖を見逃さないことが重要である（文献1）。

② 治療

糖尿病の管理目標

糖尿病の血管合併症予防のため、高血糖の是正を図るべきである。しかし高齢者、とくに後期高齢者では高血糖や糖尿病に随伴する高血圧、脂質異常をどの程度是正すると、血管合併症の発症・進展を抑制できるかを示すエビデンスは今のところない。

わが国では世界にさきがけ、高齢者糖尿病の治療ガイドラインが提唱された（文献2）。空腹時血糖値 140 mg/dl 以上、HbA1c 7%以上、糖負荷後２時間血糖値 250 mg/dl 以上、糖尿病網膜症、微量アルブミン尿症を認める例では、糖尿病性網膜症、腎症の発症・進展頻度が高く、これらに当てはまる例では、高齢者でも厳格な治療対象とすべきとしている。

高齢者糖尿病の危険因子の管理目標値を表1にまとめた。日本糖尿病学会から発表された高齢者糖尿病のガイドラインでは（文献1）、血糖管理は空腹時血糖値140 mg/dl未満、HbA1c 7%未満を目標としている（表1）。しかし高齢者糖尿病といっても、虚弱な高齢者、寝たきりの高齢者、あるいは種々の条件から血糖の適正化が困難な高齢者も多い。このような例でも、急性代謝失調、種々の合併症の進展に十分に注意して管理を行う。

食事・運動療法

高齢者でも食事・運動療法は有用な治療法である。食事療法の指導では、基本的には日本糖尿病学会の食品交換表を用いるが、患者の理解が難しい場合は、より簡易な指導要領にそった指導または介護者の教育を考慮する。

定期的な身体活動や歩行を含む運動療法は、糖尿病代謝異常の是正に有用であるばかりでなく、生命予後、大血管症の予防、ADLの維持、認知機能の低下予防にも有用である。しかし骨・関節疾患、虚血性心疾患、肺疾患、糖尿病性腎症第3期B以上を含む腎疾患、中等度以上の非増殖性糖尿病性網膜症あるいは増殖性網膜症などを有する例では、運動の実施による病態の悪化、心血管イベントの誘発などを抑制するために、運動の強度を制限する（文献1）。転倒予防のための教育と楽しく運動療法を継続できる環境整備が必要である。

■表1　高齢者糖尿病における危険因子の管理目標値（文献1,3,4より）

血糖の治療目標値

正常化を図ることが望ましい
それが困難な場合でも空腹時血糖140 mg/dl未満、HbA1cは7%未満を目標とする

血圧の治療目標値　130/80 mmHg未満

日本高血圧学会「高血圧治療ガイドライン2004」では、高齢者でも140/90 mmHg未満を降圧目標とするが、重症高血圧ではまず150/90 mmHgを暫定的目標値とした慎重な降圧が必要であるとされる。一方、血管合併症を有する糖尿病では、130/80 mmHgを降圧目標としている。高齢者糖尿病では、個々の患者の動脈硬化性病変に応じて、降圧による臓器虚血の可能性を十分に考慮した慎重な降圧を行う

脂質異常の治療目標値

血清LDLコレステロール	冠動脈疾患の1次予防：120 mg/dl未満 冠動脈疾患の2次予防：100 mg/dl未満
血清中性脂肪	150 mg/dl未満
血清HDLコレステロール	40 mg/dl以上

日本動脈硬化学会「動脈硬化性疾患診療ガイドライン2007」では、前期高齢者（65歳以上75歳未満）では上記の脂質管理を行うべきとしている。しかし後期高齢者については十分なエビデンスがなく、主治医の判断で柔軟に個々の患者に対応するのが妥当とされている

■表2　Ccr・GFRの推測式

Cockcroft-Gaultの計算式

$$Ccr\ (ml/min) = \frac{(140-年齢) \times 体重}{72 \times 血清クレアチニン値} \quad (女性：\times 0.85)$$

日本腎臓病学会慢性腎臓病対策委員会によるMDRD簡易式

$$GFR\ (mL/min/1.73\ m^2) = 0.741 \times 175 \times Age^{-0.203} \times Cr^{-1.154}$$

(女性はこれに×0.742)

薬物療法

糖尿病の薬物治療は代謝異常の是正に有用であるが、とくに低血糖に注意を要する。糖尿病治療薬による重症低血糖は高齢者、特に後期高齢者、多剤併用例、退院直後の例、腎不全例、食事摂取低下例などに発症しやすい。高齢者の低血糖では、自覚症状（交感神経症状）が軽微であり、非典型的な症状の訴え（ふらつき、落ち着かない、認知症様症状など）が少なくない。また重症低血糖は、発熱、下痢、嘔吐あるいは食欲不振時、いわゆるシックデイに発症することが多い。シックデイでの薬物量の調整は難しく、家族・介護者との連絡体制を日頃から作っておき、できるだけ早く主治医に相談するよう、シックデイ対策を教育しておくことが必要である。

長期作用型で腎排泄型のSU剤では、重症低血糖が惹起されることが多く、腎不全患者ではこの薬剤は原則として避けるべきである。高齢者では筋肉量の減少のため、血清クレアチニン値が低くなる傾向があるため、血清クレアチニン値から腎機能を推定することは危険である。Cockcroft－Gaultのクレアチニンクリアランス推定式や日本腎臓学会によるMDRD簡易式による推定GFR値で判断する（表2、文献5）。

最近のメタアナリシスによるとメトホルミン投与例における乳酸アシドーシスの発症頻度は、非投与例とほぼ同等であると報告された。しかし一般的には、80歳以上の高齢者、80歳未満であっても腎機能低下、心不全、代謝性アシドーシス、造影剤使用後48時間以内、肝障害、低酸素血症などではメトホルミン投与は原則として避けるべきとされている（文献1）。

1型糖尿病（緩徐進行型を含む）、糖尿病性昏睡、外科手術時、重症感染症などの合併例、また経口血糖降下薬で十分な血糖管理が得られない例では、インスリン療法を行う。投与法には高齢者にとってシンプルな持効型インスリンの一日一回投与と超即効型インスリンの毎食前投与という対極に位置する2つの考え方がある。高齢者糖尿病でどちらの投与法が糖尿病コントロールに有益であるかを示すエビデンスはない。実際にはインスリン自己注射を本人または介護者に委ねられるかがポイントとなることが多い。介護保険サービスの訪問看護などの利用も考慮する。

③ 高齢者糖尿病で特徴的な問題点

複数の血管合併症、特に大血管症に加えて、他疾患の合併、ADL や認知機能低下などのために、自立した生活、糖尿病の自己管理が高頻度に困難となる（図 1）。

なかでも認知症は高齢者医療の最大の課題である。糖尿病では認知機能が低下し、高齢者糖尿病は血管性認知症、アルツハイマー病の危険因子であることが明らかにされている（文献 6）。糖尿病における脳血管障害、高血圧、脂質異常あるいは高インスリン血症、高血糖の持続が認知機能の低下の原因になると考えられている。したがって血糖のみならず血圧、血清脂質、体重などの適正化、さらに生活・運動習慣を改善することで、血管合併症の発症・進展のみならず、他疾患、認知症、ADL の低下などの発症、悪化予防に努める。

QOL の維持・向上が特に重要である。QOL の低下は脳卒中の危険因子であり、うつ状態は QOL を低下させ、入院や死亡のリスクとなる。尿失禁、インスリン治療や厳しい生活規制も QOL を低下させることがある。このため糖尿病状態のみならず、個々の患者の身体的、精神・心理的、社会的背景を総合的に評価（CGA）し、それぞれに最適と考えられる治療を計画する（表 3）。独居高齢者、虚弱な高齢者糖尿病では、介護保険サービスの積極的利用で、治療コンプライアンスの向上を図る。

■図 1　高齢者糖尿病の合併症と生活機能障害

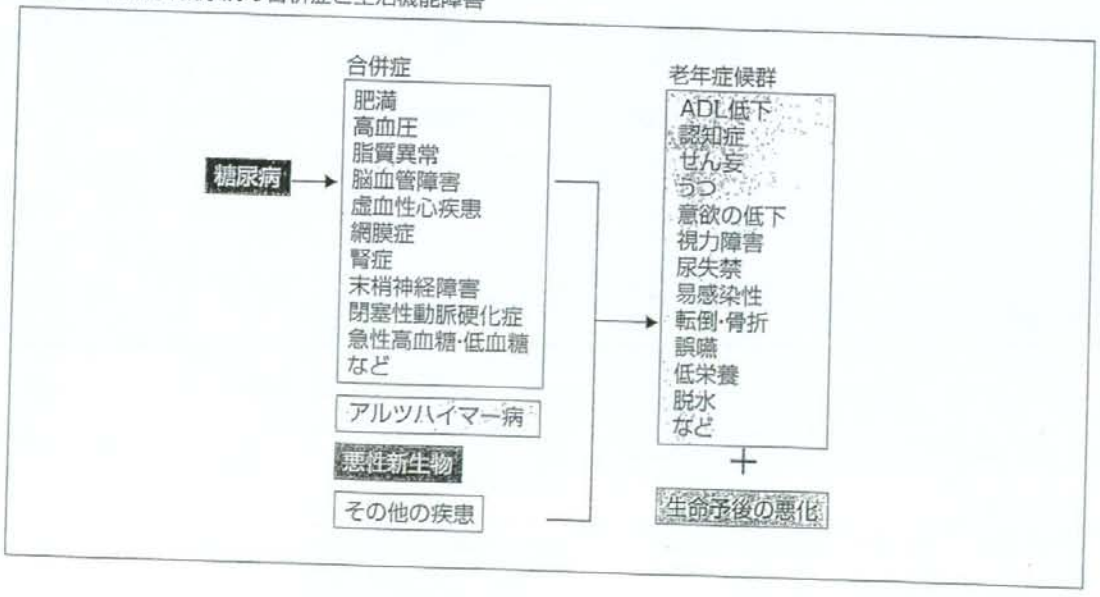

■表 3　高齢者糖尿病において評価すべきこと

・糖尿病の状態

病型、罹病期間、インスリン分泌・感受性、血糖コントロール、肥満、高血圧、脂質異常、血管合併症など

・他疾患の合併

他疾患の有無（心疾患、骨・関節疾患、悪性新生物など）、生命予後

・視力・聴力・尿失禁・コミュニケーション

・日常生活動作

基本的 ADL　　手段的 ADL

・精神・神経機能

認知機能（改訂長谷川式簡易知能検査、ミニメンタルテストなどで評価）うつ状態（Geriatric depression scale: GDS15 などで評価）意欲（鳥羽式スケールなどで評価）

・社会・経済的状況

家族構成とキーパーソン、住居、経済状況、介護保険の利用

④ 専門医紹介のポイント

◉糖尿病の急性発症または血糖コントロール増悪時

インスリン療法の導入は原則的に入院とする。体重減少を伴う例では、悪性腫瘍を合併することが少なくない。薬剤性、糖尿病以外の原因についても検査する。

◉急性代謝失調（高血糖高浸透圧症候群・糖尿病性ケトアシドーシス、遷延性低血糖、シックデイ）

◉血管合併症の検査（脳、心、下肢動脈、腎、眼、末梢神経障害など）

血管合併症の急性発症時には直ちに該当科での治療を要する。高齢者糖尿病では動脈硬化性疾患の合併頻度が高く、無症候性の脳梗塞、心筋虚血が多いことから、全身の血管障害の検査を積極的に行う。

◉高齢者に特有の合併症（認知症、うつ、骨病変・転倒、尿失禁など）

合併症、生活機能障害は、自立した療養を阻害する（図 1）。とくに後期高齢者では、認知症の早期発見、転倒・骨折の予防が重要である。

（櫻井　孝）

Kobe J. Med. Sci., Vol. 53 No. 6, pp. 317-326, 2007

Loss of CO_2-induced Distensibility in Cerebral Arteries with Chronic Hypertension or Vasospasm after Subarachnoid Hemorrhage

SEIJI NAKAJIMA[1], TAKESHI KONDOH[1], AKITSUGU MORISHITA[1], HARUO YAMASHITA[1], EIJI KOHMURA[1], TAKASHI SAKURAI[2], KOICHI YOKONO[2], and KEIJI UMETANI[3]

Department of [1]Neurosurgery and [2]Internal and Geriatric Medicine, Graduate School of Medicine, Kobe University, Kobe, Japan

[3]Japan Synchrotron Radiation Research Institute, SPring-8, Sayo-gun, Hyogo, Japan

Received 27 February 2007 /Accepted 9 March 2007

Key Words: angiography, hypercapnia, spontaneously hypertensive rat, subarachnoid hemorrhage, synchrotron radiation, vasospasm

Abbreviations: ICA, internal carotid artery; MCA, middle cerebral artery; ACA, anterior cerebral artery; ECA, external carotid artery; CCA, common carotid artery; MAP, mean arterial pressure; PCA, posterior cerebral artery; BA, basilar artery

We developed a rat cerebral angiography system using monochromatic synchrotron radiation X-rays at SPring-8, a third generation synchrotron radiation facility. Using new technique, we assessed the distensibility of major trunk arteries after subarachnoid hemorrhage (SAH) in normotensive and hypertensive rats. Twenty-five adult Wistar Kyoto rats (WKY) and fourteen stroke-prone spontaneously hypertensive rats (SHR) were prepared SAH by double hemorrhage injection method into cisterna magna. Angiography was performed on day 7 and was repeated three times in each rat before and after loading of hypercapnia at 100-120 mmHg of $PaCO_2$. The diameters of major trunk vessels were assessed. Light microscopic observation of artery lumen and wall were also performed. Angiographical vasospasm was demonstrated in basilar artery in WKY with 66 % reduction in diameter of control. In ICA and other major trunk in WKY and all the arteries in SHR did not demonstrate vasospasm. SHA resulted in loss of hypercapnia-induced distention in BA of WKY. In SHR, the distensibility was impaired regardless of hemorrhage. Histological study demonstrated basilar artery in WKY thickened at 184 % after SAH and became similar to non-hemorrhagic SHR. ICA in WKY and both BA and ICA in SHR were unchanged in wall thickness before and after SAH. High quality angiography demonstrated deteriorated distensibility in chronic hypertension or SAH-induced spastic vessels.

Subarachnoid hemorrhage (SAH) is often associated with a delayed vasospasm that is a major course of disability in patients after cerebral aneurysm rupture. Many researchers have used rodents to study the pathogenesis of cerebral vasospasm after SAH because small animals are less expensive and easy to handle. Rat models were developed in which blood was injected directly into the cisterna magna (3, 24). The degree of vasospasm is determined by measurement of the vessel diameters and direct observation through cranial

Phone: +81-78-382-5966 Fax: +81-78-382-5979 e-mail: tkondo@med.kobe-u.ac.jp

bone window was used initially (2). Subsequently, angiography has been reported in rat SAH model, however, it is very difficult because of the small size of the animal. Furthermore, physiological change cannot be characterized as it has in models using other larger species.

Recently, we have developed a microangiography system using monochromatic synchrotron radiation X-rays at SPring-8, a third generation synchrotron radiation facility. With this system at SPring-8, high spatial resolution of 8 μm has been achieved using phantoms. We have firstly applied this system for cerebral microangiography in rats and mice (9, 13, 16, 25). In the present study, we have focused on in vivo assessment of spastic rat cerebral arteries after SAH. Impaired autoregulation of the cerebral blood flow has been known in rat SAH model between 2 and 5 days after SAH (20). This study was done with133-Xenon injection into carotid artery and reflected pathogenesis of small arteriole in the cortex. The major artery trunks, that are targets of interventional approach in patients, were not shown yet in previous studies. Using microangiography technique, we studied the change of distensibility of those major artery trunks by loading systemic hypercapnia.

Secondly, we studied the effects of chronic hypertension on vasospasm using spontaneously hypertensive rats (SHR). Chronic hypertension in SHR induces thick media in cerebral arteries in comparison with normotensive rats (15) and may affect the spastic change as well as distensibility in systemic hypercapnia. Although aging is known to increase the degree of vasospasm after SAH in rabbits, studies with chronic hypertension has not been done yet.

MATERIALS AND METHODS

Imaging System and Animal Preparation

All experimental procedures followed the guidelines for animal experimentations at Kobe University Graduate School of Medicine. The imaging was performed at the 2nd optical hatch of BL28B2 beamline at SPring-8 (Japan Synchrotron Radiation Research Institute) in Hyogo, Japan. Details of the imaging system used in the present study were, in part, previously described (13, 16).

Adult Wistar Kyoto rat (WKY, n=25) and adult SHR (n=14), weighting between 450 and 600g, aged 6 months, were used. The method to produce SAH is based on a double hemorrhage injection method. On day 0, rats were anesthetized with pentobarbital sodium (50 mg/kg, i.p.) and allowed to breath spontaneously. Under sterile condition, rats were held in a 20° head down in a stereotaxic frame and the atlano-occipital membrane was exposed. A 27-gauge needle bent at the tip for a length of 2 mm was carefully inserted into the cisterna magna. On day 2, rats were anesthetized again and a second SAH was induced as described above. On day 7, imaging study was performed under pentobarbital sodium (50 mg/kg, i.p.) anesthesia, which has been reported in our previous reports (13, 16).

Experimental Protocol

After the animal preparation was completed, the PE-50 tube inserted into the ECA was connected to an automated injector (Nihon Koden, Japan) that was programmed to reproducibly deliver nonionic contrast media (Iomeprol) at 0.2 ml / 0.4 sec for ICA imaging and 0.5 ml / 1.0 sec for BA. This injection volume and speed were determined based on our pilot study, in which different volumes of the contrast media were injected at different injection rates to obtain the most acceptable and physiological images. Arterial blood gases were checked before the first imaging. The first angiogram was performed to estimate the basal tone of the vessels. We allowed at least 3-min intervals between angiograms to reestablish physiological blood flow before each angiographic study.

The inhalation of CO_2 at 12-15 % mixed in air was performed for 6 minutes. An angiogram, at the end of inhalation, was then performed. The arterial blood gases were analyzed and the inhalation was returned to normal air. An additional angiogram was performed at 10 min under normocapnia, and the arterial blood gases were analyzed. Rats were divided into four subgroups; a) WKY with SAH (n=17), b) WKY without SAH (n=5), c) SHR with SAH (n=9), d) SHR without SAH (n=8). Rats in group b) and d) were as control in which saline was injected into cisterna magnum instead of autologous blood.

Image Analysis

The images were stored digitally. The initial acquisition time for an image was 30 images per second. To make the subtraction images, ten original images were added and subtracted by the pre-infusion image. The vessel diameter was measured semiautomatically on the digital image with readymade software (Image ProPlus, U.S.A.) combined with a program developed for this study. A short temporary axis was delineated by hand at the vessels specified for measurement. The axis was delineated within 0.5 mm after branching for PCA, MCA and ACA. For ICA, the axis was in the middle of the segment between PCA and MCA. BA was measured at two points of one third proximal and one third distal. The density profile perpendicular to the temporary axis was calculated and distance between these two peaks of phase refractions of X-ray on the border of vessel wall was measured as a diameter of the vessel.

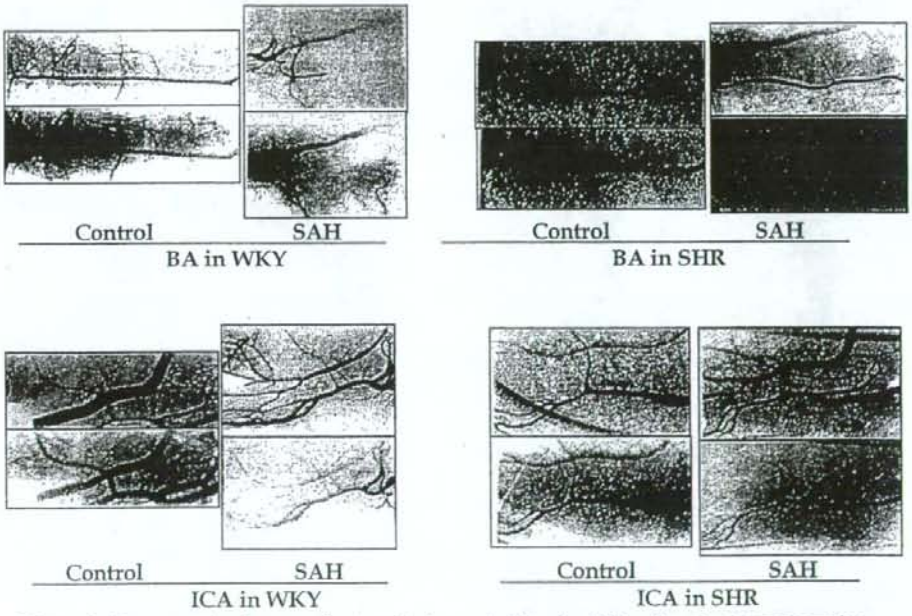

Figure 1: Representative images of rat cerebral vessels taken by SPring-8 and micorangiography technique. Uppper: normocapnia, lower: hypercapnia. BA: basilar artery, ICA: internal carotid artery, SHR: spontaneously hypertensive rat, WKY: Wistar Kyoto rat, SAH: subarachnoid hemorrhage.

Morphometric study

After angiography, rats were killed by overdose anesthesia and decapitated. Rats were perfused transcardially by 4% parahormaldehyde in phosphate buffer for 30 minutes. Brain were removed and soaked in 10 % parahormaldehyde for 7days. After paraffin embedding, slices containing basilar artery and internal carotid artery was made at the thickness of 10 μm and stained with hematoxylin and eosin. The internal diameter and wall thickness of the arteries were measured using a digitized image analysis system. The thickness was defined as the distance from the luminal surface to the outer border of the media at four different points.

Statistics

Data are presented as means +/- S.E.. An unpaired Student *t* test was used to detect significant differences when two groups were compared. Statistical differences among group means were determined by one-way ANOVA with repeated measures, followed by a post hoc comparison. A value of $P< 0.05$ was considered to be statistically significant.

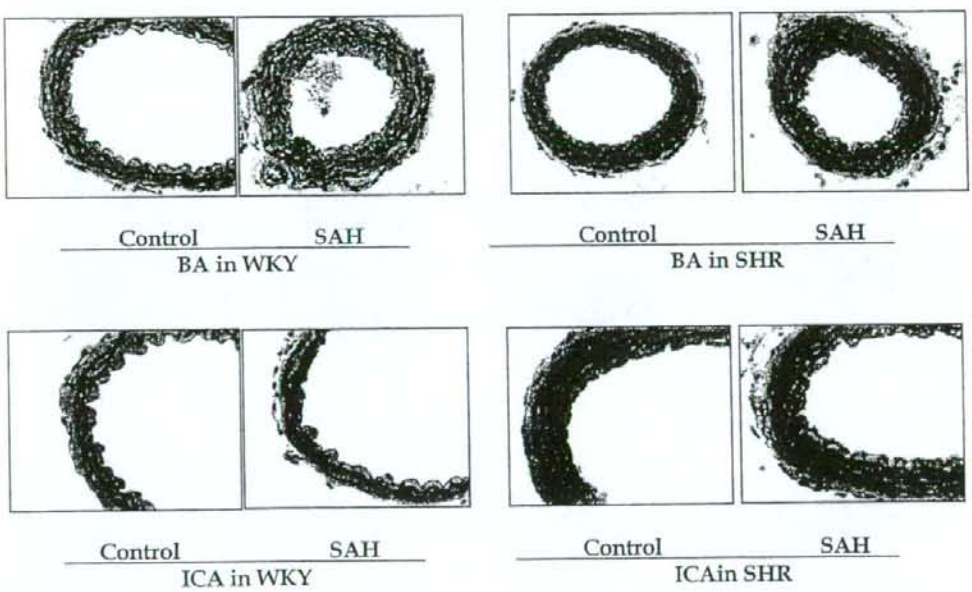

Figure 2: Histological demonstration of cross section in basilar arteries and internal carotid arteries.

RESULTS

With our experimental setting of 0.2 ml injection, the posterior fossa was not filled by the contrast media indicating selective ICA angiography was performed. Within the radiation field of 3 x 7.3 mm, the images of major trunk vessels of ICA from the entry point to intracranial space, PCA, MCA and ACA were consistently obtained. The posterior choroidal artery, the large branch of PCA was also within the field but it was always associated with overlapping images of thalamic branches in the axial view and this made analysis impossible. The image of posterior communication artery arising from the PCA was occasionally obtained by selective ICA angiography but mostly faint.

The vessel diameters of rats without SAH (SAH(-)) and rats with SAH(SAH(+)) measured by angiography were summarized in Table 1. In SAH(-) rats, the diameters of BA were significantly narrower in SHR than in WKY (132 μm vs.248 μm at proximal and 102 μm vs. 274 μm at distal; $p < 0.05$) and other major trunk vessels did not significantly differ between WKY and SHR. In SAH(+) rats, significant vasospasm was observed in BA of WKY (64-66 % of SAH(-)). Other major trunk vessels in SAH(+) WKY and all of the major trunk vessels in SAH(+) SHR-SP had no spastic changes (81-139 % of SAH(-)).

By loading CO_2, all of the trunk vessels in SAH(-) WKY demonstrated significant dilatation (125 –169 % of pre-CO_2 values for each) (Table 2). This dilatation ability was lost after SAH except PCA. In SHR, both SAH(-) and SAH(+) did not demonstrated vasodilatation by CO_2 loading at all.

The histological measurement of ICA and BA before SAH demonstrated significant narrower diameter in SHR compared with WKY (110 μm vs. 153 μm in BA and 218 μm vs. 297 μm in ICA) as shown in Table 3. SAH-induced narrowing of the vessels was not observed histologically in all. The measurement of arterial wall thickness demonstrated that in SAH(-) rats, both BA and ICA had significantly thicker wall in SHR compared with WKY (29.6 μm vs. 19.2 μm in BA and 33.3 μm vs. 29.2 μm in ICA). SAH-induced-pathological change was observed only in BA of WKY, in which arterial wall significantly thickened by SAH (181 % of SAH(-)). This thickened value of the diameter in BA of WKY was comparable to BA of SHR.

Table 1. Comparative measurments in WKY and SHR with subarachnoid hemorrhage

	vessel diameter (μm)			
	SAH(-)	SAH(+)	Spasm (%)	p Value
Basilar A.(proximal)				
WKY	248±21.3	164±34.7	66	0.02
SHR	132±33.1	149±32.3	112	NS
Basilar A.(distal)				
WKY	274±26.7	176±36.1	64	0.02
SHR	102±41.8	124±36.1	121	NS
ICA				
WKY	319±28.1	360±39.2	113	NS
SHR	340±27.7	306±37.5	99	NS
MCA				
WKY	214±30.3	235±21.5	109	NS
SHR	218±15.9	217±14.7	99	NS
ACA				
WKY	255±20.3	208±27.1	81	NS
SHR	226±18.6	226±21.2	100	NS
PCA				
WKY	180±28.5	251±15.0	139	NS
SHR	220±46.6	212±26.7	97	NS

Table 2. CO2 induced distention of trunk vessels in the chronic vasospasm

	WKY				SHR			
	SAH(-)		SAH (+)		SAH(-)		SAH (+)	
	mean±SE (%)	p value	mean±SE (%)	p value	mean±SE (%)	p value	mean±SE (%)	p value
Basilar A.(proximal)								
pre	238±21.3 (100)	P=0.04	164±34.7 (100)	NS	132±33.1 (100)	NS	148±32.3 (100)	NS
post	294±27.9 (125)		151±35.1 (99.7)		172±46.3 (130)		165±37.5 (11.5)	
rec/10min	236±37.7 (99.1)		145±51.6 (88.7)		155±48.2 (117)		152±46.6 (102)	
Basilar A.(distal)								
pre	268±26.7 (100)	P=0.03	176±36.1 (100)	NS	102±41.8 (100)	NS	124±36.1 (100)	NS
post	368±43.2 (137)		161±42.5 (91.1)		128±56.5 (133)		141±54.8 (114)	
rec/10min	294±51.4 (108)		140±49.1 (79.2)		170±49.5 (133)		114±69.8 (91.7)	
ICA								
pre	319±28.1 (100)	P=0.0001	390±27.4 (100)	NS	340±27.8 (100)	NS	306±37.5 (100)	NS
post	385±23.4 (121)		455±34.7 (117)		353±29.6 (104)		382±48.8 (125)	
rec/10min	338±37.5 (106)		375±26.2 (96.1)		317±43.3 (93.1)		234±9.3 (76.4)	
MCA								
pre	214±22.4 (100)	P=0.01	235±21.5 (100)	NS	218±15.9 (100)	NS	216±14.7 (100)	NS
post	298±19.5 (139)		229±40.3 (97.4)		250±26.5 (115)		245±13.4 (113)	
rec/10min	201±26.1 (93.9)		223±40.8 (94.9)		210±15.3 (96.3)		158±5.8 (72.8)	
ACA								
pre	255±20.3 (100)	P=0.04	226±22.7 (100)	NS	226±18.6 (100)	NS	226±21.2 (100)	NS
post	282±32.4 (110)		265±24.2 (117)		230±20.8 (102)		274±19.4 (121)	
rec/10min	260±23.1 (102)		205±22.3 (87.2)		200±15.3 (88.5)		182±24.8 (80.5)	
PCA								
pre	180±28.5 (100)	P=0.01	251±15.0 (100)	p=0.007	220±46.6 (100)	NS	212±26.7 (100)	NS
post	226±19.7 (126)	P=0.007	313±18.4 (125)		207±41.0 (93.9)		258±18.8 (122)	
rec/10min	226±8.4 (145)		257±24.3 (102)		160±30.6 (72.7)		166±28.9 (78.1)	

Table 3. Comparative measurments in normal rats and SHR with subarachnoid hemorrhage

	WKY			SHR		
	SAH(-)	SAH(+)	p Value	SAH(-)	SAH(+)	p Value
Basilar A						
vessel wall(μm)	19.16±0.17	34.82±1.28	p=0.002	29.58±0.67	31.25±0.98	NS
vessel lumen(μm)	153.33±6.89	151.79±9.57	NS	110±7.29	83.33±5.00	NS
ICA						
vessel wall(μm)	29.16±0.83	29.29±1.08	NS	33.33±0.33	35.25±0.56	NS
vessel lumen(μm)	296.67±32.0	272.5±13.08	NS	217.5±10.79	197±14.26	NS

DISCUSSION

Angiographical Assessment of Vasospasm in Rodents

Measurements of rat cerebral arteries after subarachnoid hemorrhage have been reported using angiography (3, 8, 11, 17, 27), and observation with a cranial window (18, 22, 23). By mammographic equipment or selective biplane digital subtraction angiography systems, recent studies using rodents showed availability of measuring the vessel diameters with or without spasms (11, 26).

Magnification of the vessels using a mammography suggests the possibility of visualizing the small cerebral vessels (11, 12, 17). The small focus technique provides high geometric magnification with longer film - focus distance. This technique is especially useful in combination with digital subtraction techniques. They demonstrated the ability to view rat cerebral trunk arteries and some extracranial arteries including superior and inferior ophthalmic arteries, although the vessel diameters were not measured. The theoretical magnification of the mammography was suggested to be x 250 in the literature, however, one

concern with magnification increases, is radiation scattering which makes the margins of vessel image blurry.

Regarding the time resolution for rat cerebral angiography, some studies used anterograde injection of the contrast media by placing the cannula in CCA or ICA, thus the ipsilateral blood flow in ICA was disrupted (11, 12). With this preparation, the volumes of injected contrast media were between 0.2 to 0.3 ml. The obtained images showed cross filling of the contrast media to the whole contralateral hemisphere as well as the posterior fossa, suggesting that normal intracranial blood flow was absolutely changed at the time of imaging. Others used retrograde injection via the ECA to the CCA (17). An external carotid perfusion loop allows for the introduction of the contrast medium without changing perfusion pressure or flow in the cerebral hemisphere. However, the injection volume of the contrast media was as high as 0.5 ml and only a single angiography was performed in one experimental setting.

In the present study, we demonstrated the ability to obtain rat cerebral microangiograms using synchrotron radiation. Selective microangiography of hemispheric brain clearly showed not only the images of major trunk vessels but also of vessels less than 100 μm in diameter. The subtraction images were obtained every 0.33 sec and microangiography repeated up to five times in each rat, which is in contrast with previous studies where only two imagings could be done. This high quality of microangiography has not been reported by current conventional method of imaging. We believe that this can be obtained only by the combination of highly monochromatized SR and a new X-ray SATICON camera.

We found that the absolute value of vessel diameter in our studies was smaller than previous studies in the rat brain, in which angiography using mammography measured the diameter of the MCA in rat at 305-350 μm (11, 17). The diameter of the MCA in our study was at 201 +/- 20 μm in WKY. This diameter is close to that found in a histological study (15, 20) and we think, therefore, that our study is likely more accurate. Magnified images in mammography may have scattering radiation around the contrast media resulting in obscure margins and inaccurately larger diameter of the vessels. A large injection volume of the contrast media or proximal blocking of the ICA due to the catheter placement might cause the enlargement of the vessels that can not be detected by conventional methods used in previous studies.

Chronic Hypertension and Distensibility of Cerebral Arteries

In WKY, we observed vasospasm in basilar artery after SAH at 66% of pre-SAH diameter. The vasospasm was not observed in ICA, MCA, ACA and PCA. Actually, ICA and PCA showed a tendency of enlargement of the vessels after SAH, although which was not statistically significant (ICA: from 319 μm to 360 μm, PCA: from 180 μm to 251 μm). Interestingly, similar pattern of enlargement in ICA and PCA were observed in comparison between normotensive WKY and hypertensive SHR (ICA: 319 μm to 340 μm, PCA: 180 μm to 220 μm). We speculate that after SAH in WKY, ICA and PCA might be enlarged due to compensatory dilatation for severely affected spastic basilar artery that was mostly affected by SAH by blood injection into posterior cranial fossa. Similarly, in SHR, the basilar artery might be mostly affected because other major vessels have a collateral blood flow via the external carotid arteries.

We have demonstrated that the vasospasm was absent in basilar artery of the SHR. We suspect that the reason for absence of vasospasm was, at least in part, due to morphological change of vessel wall. In comparison of the thickness of basilar artery wall between WKY and SHR, SHR was significantly thicker than WKY (30 μm in SHR vs. 19 μm in WKY). Not only simply thick wall but also morphological changes of medial smooth muscle cells

and blood brain barrier have been reported in SHR (1, 15). Taken together, pre-existing affected distensibility in SHR might result in lack of spastic change after SAH. This may be also responsible for our observation of lack of distention by hypercapnia in SHR. The distensibility of affected vessels can be quantified only by high-resolution imaging. Regarding the impact of chronic hypertension on the distensibility of cerebral vessels, previous study using SHR and laser Doppler measurement of cerebral blood flow has been reported that pressure-dependent constriction of cerebral vessels was attenuated and lost after stroke (21). By hypercapnia, cerebral blood flow measurement by hydrogen clearance method resulted in no significant difference of the vasodilation between normotensive rats and hypertensive rats (6). Those previous studies were based on relative blood flow changes and direct measurement of the vessel diameter has never been performed. With large experimental animals, various studies have been reported but those were all non-pathological condition and no study could be done with chronic hypertension (4, 5, 7). Our study showed that major trunk vessels in SHR were less affected by SAH than in WKY, indicating that the degree of vessel damage is already maximized in SHR, leading high vulnerability. Similar result was obtained using young and aged rabbit with SAH (14).

Clinical implication of the present data

Our results in this study were mimicking of clinical observation in several points (10). Firstly, location of SAH clot is a key of induction of vasospasm, which is commonly observed in SAH patients and we found similar localized vasospasm in rodent. Secondly, the mortality of SHR after SAH was recognized high as two out of nine rats whereas zero in WKY. Pre-existing deteriorated autoregulation of the cerebral blood flow in SHR probably lead low blood perfusion in brain stem, resulting fetal ischemia under circumstances of high intracranial pressure with SAH. Thirdly, autoregulation of cerebral blood flow is affected even in normotensive WKY, indicating maintaining of systemic blood pressure is essential to prevent delayed ischemic damage after SAH. Impaired endothelium-dependent relaxation has been discussed recently as a main reason of such pathogenesis of distensibility (26). To evaluate such a mechanisms, not only a simple measurement of vessel diameters but also imaging studies like microangiography using vasodilator is useful.

ACKNOWLEDGMENT

This work was supported in part by Grant-in-Aid for Scientific Research (C)(2)(13671435) to T.K. and from the Ministry of Education, Science, Sports, and Culture of Japan and by a grant for Gerontological Research to T.S. from Novartis Foundation.

REFERENCES

1. **Amenta F., Ferrante F., Sabbatini M., and Ricci A.** 1994. Quantitative image analysis study of the cerebral vasodilatory activity of nicardipine in spontaneously hypertensive rats. Clin Exp Hypertens. **16**: 359-371.
2. **Barry K.J., Gogjian M.A., and Stein B.M.** 1979. Small animal model for investigation of subarachnoid hemorrhage and cerebral vasospasm. Stroke. **10**: 538-541.
3. **Delgado T.J., Brismar J., and Svendgaard N.A.** 1985. Subarachnoid haemorrhage in the rat: angiography and fluorescence microscopy of the major cerebral arteries. Stroke **16**: 595-602.
4. **Diringer M.N., Heffez D.S., Monsein L., Kirsch J.R., Hanley D.F., and Traystman R.J.** 1991. Cerebrovascular CO2 reactivity during delayed vasospasm in a canine model of subarachnoid hemorrhage. Stroke **22**: 367-372.

5. **Diringer M.N., Kirsch J.R., and Traystman R.J.** 1994. Reduced cerebral blood flow but intact reactivity to hypercarbia and hypoxia following subarachnoid hemorrhage in rabbits. J Cereb Blood Flow Metab **14**: 59-63.
6. **Heinert G., Casadei B., and Paterson D.J.** 1998. Hypercapnic cerebral blood flow in spontaneously hypertensive rats. J Hypertens. **16**: 1491-1498.
7. **Ishiguro M., Puryear C.B., Bisson E., Saundry C.M., Nathan D.J., Russell S.R., Tranmer B.I., and Wellman G.C.** 2002. Enhanced myogenic tone in cerebral arteries from a rabbit model of subarachnoid hemorrhage. Am J Physiol Heart Circ Physiol **283**: H2217-2225.
8. **Kader A., Krauss W.E., Onesti S.T., Elliott J.P., and Solomon R.A.** 1990. Chronic cerebral blood flow changes following experimental subarachnoid hemorrhage in rats. Stroke. **21**: 577-581.
9. **Kidoguchi K., Tamaki M., Mizobe T., Koyama J., Kondoh T., Kohmura E., Sakurai T., Yokono K., and Umetani K.** 2006. In vivo X-ray angiography in the mouse brain using synchrotron radiation. Stroke.**37**: 1856-1861.
10. **Lanzino G., Kassell N.F., Germanson T.P., Kongable G.L., Truskowski L.L., Torner J.C., and Jane J.A.** 1996. Age and outcome after aneurysmal subarachnoid hemorrhage: why do older patients fare worse? J Neurosurg **85**: 410-418.
11. **Longo M., Blandino A., Ascenti G., Ricciardi G.K., Granata F., and Vinci S.** 2002. Cerebral angiography in the rat with mammographic equipment: a simple, cost-effective method for assessing vasospasm in experimental subarachnoid haemorrhage. Neuroradiology **44**: 689-694.
12. **Luedemann W., Brinker T., Schuhmann M.U., von Brenndorf A.I., and Samii M.** 1998. Direct magnification technique for cerebral angiography in the rat. Invest. Radiol. **33**: 421-424.
13. **Morishita A., Kondoh T., Sakurai T., Ikeda M., Bhattacharjee A.K., Nakajima S., Kohmura E., Yokono K., and Umetani K.** 2006. Quantification of distension in rat cerebral perforating arteries. Neuroreport. **17**: 1549-1553.
14. **Nakajima M., Date I., Takahashi K., Ninomiya Y., Asari S., and Ohmoto T.** 2001. Effects of aging on cerebral vasospasm after subarachnoid hemorrhage in rabbits. Stroke **32**: 620-628.
15. **Nordborg C., Fredriksson K., and Johansson BB.** 1985.The morphometry of consecutive segments in cerebral arteries of normotensive and spontaneously hypertensive rats. Stroke. **16**: 313-320.
16. **Oizumi X.S., Akisaki T., Kouta Y., Song X.Z., Takata T., Kondoh T., Umetani K., Hirano M., Yamasaki K., Kohmura E., Yokono K., and Sakurai T.** 2006. Impaired response of perforating arteries to hypercapnia in chronic hyperglycemia. Kobe J Med Sci. **52**: 27-35.
17. **Piepgras A., Thome C., and Schmiedek P.** 1995. Characterization of an anterior circulation rat subarachnoid hemorrhage model. Stroke **26**: 2347-2352.
18. **Quan L., and Sobey C.G.** 2000. Selective effects of subarachnoid hemorrhage on cerebral vascular responses to 4-aminopyridine in rats. Stroke **31**: 2460-2465.
19. **Rasmussen G., Hauerberg J., Waldemar G., Gjerris F., and Juhler M.** 1992. Cerebral blood flow autoregulation in experimental subarachnoid haemorrhage in rat. Acta Neurochir (Wien). **119**: 128-133.
20. **Rieke G.K.** 1987. Thalamic arterial pattern: an endocast and scanning electron microscopic study in normotensive male rats. Am. J. Anat. **178**: 45-54.
21. **Smeda J.S., VanVliet B.N., and King S.R.** 1999.Stroke-prone spontaneously

hypertensive rats lose their ability to auto-regulate cerebral blood flow prior to stroke. J Hypertens. **17**: 1697-1705.

22. **Sobey C.G., Heistad D.D., and Faraci F.M.** 1996. Effect of subarachnoid hemorrhage on dilatation of rat basilar artery in vivo. Am J Physiol **271**: H126-132.
23. **Sobey C.G., Heistad D.D., and Faraci F.M.** 1997. Effect of subarachnoid hemorrhage on cerebral vasodilatation in response to activation of ATP-sensitive K+ channels in chronically hypertensive rats. Stroke **28**: 392-396.
24. **Solomon R.A., Antunes J.L., Chen R.Y., Bland L., and Chien S.** 1985. Decrease in cerebral blood flow in rats after experimental subarachnoid hemorrhage: a new animal model. Stroke. **16**: 58-64.
25. **Tamaki M., Kidoguchi K., Mizobe T., Koyama J., Kondoh T., Sakurai T., Kohmura E., Yokono K., and Umetani K.** 2006. Carotid artery occlusion and collateral circulation in C57Black/6J mice detected by synchrotron radiation microangiography. Kobe J Med Sci. **52**: 111-118.
26. **Weidauer S., Vatter H., Dettmann E., Seifert V., and Zanella F.E.** 2006. Assessment of vasospasm in experimental subarachnoid hemorrhage in rats by selective biplane digital subtraction angiography. Neuroradiology **48**: 176-181.
27. **Yamamoto S., Nishizawa S., Tsukada H., Kakiuchi T., Yokoyama T., Ryu H., and Uemura K.** 1998. Cerebral blood flow autoregulation following subarachnoid hemorrhage in rats: chronic vasospasm shifts the upper and lower limits of the autoregulatory range toward higher blood pressures. Brain Res **782**: 194-201.

Microvascular Research 77 (2009) 230–233

Contents lists available at ScienceDirect

Microvascular Research

journal homepage: www.elsevier.com/locate/ymvre

Short Communication

Dilation of perforating arteries in rat brain in response to systemic hypotension is more sensitive and pronounced than that of pial arterioles Simultaneous visualization of perforating and cortical vessels by in-vivo microangiography

Hiroshi Yoshino [a], Takashi Sakurai [a,*], Ximena-Sayuri Oizumi [a], Taichi Akisaki [a], XiaoNan Wang [a], Koichi Yokono [a], Takeshi Kondoh [b], Eiji Kohmura [b], Keiji Umentani [c]

[a] Department of Internal and Geriatric Medicine, Kobe University Graduate School of Medicine, 7-5-1 Kusunoki-cho, Chuo-ku, Kobe 650-0017, Japan
[b] Department of Neurosurgery, Kobe University Graduate School of Medicine, Japan
[c] Japan Synchrotron Radiation Research Institute, SPring-8, Sayo-gun, Hyogo, Japan

ARTICLE INFO

Article history:
Received 25 March 2008
Revised 26 September 2008
Accepted 29 September 2008
Available online 18 October 2008

Keywords:
Autoregulatory vascular dilatation
Perforating artery
Pial artery
Hypotension
Rat

ABSTRACT

Autoregulatory responses of perforating arteries play a key role in the maintenance of microcirculation of the deep brain regions. The aim of this study was to test our hypothesis that autoregulatory vasodilatation of perforating arteries is more effective than that of cortical arteries. We performed cerebral microangiography in adult Wistar rats using monochromatic synchrotron radiation at SPring-8 and for the first time radiographically visualized perforating arteries and cortical arteries simultaneously in a single view. In response to hypotension induced by arterial bleeding, both arteries showed significant vasodilatation. Steady-state responses of increments in caliber to stepwise hypotension revealed that perforating arteries exhibited significant vasodilatation at blood pressure below 80–99 mm Hg. Cortical arteries, on the other hand, showed a gradual and smaller vasodilatation beginning at 60–79 mm Hg. For the lowest blood pressure range at 40–59 mm Hg, the smallest arteries with a diameter of 20–40 μm showed maximal dilation in both groups, but perforating arteries showed significantly larger dilatation (185.0% of baseline diameter) than cortical arteries (152.7%; $P=0.003$). Our results indicate that vasodilatation of perforating arteries is more sensitive and pronounced in response to systemic hypotension than that of pial arteries, which explains how cerebral microcirculation is maintained efficiently in the deep brain regions.

Introduction

Perforating arteries are terminal vessels located deep in the ventral brain area. They directly emerge from the main cerebral trunks without collateral flow with adjacent arteries. Perforating arteries are particularly important because they supply blood to vulnerable parts of brain structures, e.g., basal ganglia, thalamus and hippocampus. Pial arterioles are located on the cortical surface and are richly anastomosed, not only among themselves, but also with the branches from the external carotid artery (ECA). Such rich anastomosis can compensate for reduction in local perfusion during hypotension.

Autoregulation of cerebral blood flow (CBF), the tendency for blood flow to remain constant despite changes in arterial perfusion pressure, is a crucial mechanism for the maintenance of cerebral circulation. This autoregulation of blood flow is accomplished via constriction of cerebral blood vessels as the pressure rises and vasodilatation as the blood pressure declines (Kontos et al., 1978; Faraci and Heistad, 1998). Autoregulatory response of perforating arteries plays a key role in sustaining microcirculation of the deep brain regions and its disruption may be involved in the pathogenesis of small-vessel diseases such as lacunar infarction and leukoaraiosis (Jorgensen et al., 1994; Molina et al., 1999). However, so far it has not been possible to examine autoregulatory adjustments of perforating arteries radiographically because of their deep-seated anatomical location and small size. Nor has any comparative study been made of perforating arteries and pial vessels.

We recently developed a novel cerebral angiography procedure for rodents using monochromatic synchrotron radiation X-rays at SPring-8 and obtained images of cerebral perforating arteries (Morishita et al., 2006; Kidoguchi et al., 2006; Oizumi et al., 2006). In the study presented here, we improved this procedure to visualize rat perforating and cortical arteries simultaneously in a single view. We then used this method to test the hypothesis that, after induced hypotension, perforating arteries distend more efficiently than pial arteries to maintain constant blood supply to the deep brain regions.

* Corresponding author. Fax: +81 783825919.
E-mail address: sakurai@med.kobe-u.ac.jp (T. Sakurai).

0026-2862/$ – see front matter © 2008 Published by Elsevier Inc.
doi:10.1016/j.mvr.2008.09.011

Material and methods

This study used nine 6-month-old male Wistar rats weighing 400–450 g. All of our experimental procedures were in accordance with the guidelines for animal experiments of Kobe University. The cerebral microangiography for rat brain used ultra-bright and monochromatic X-rays at the third-generation synchrotron radiation center SPring-8. Details of the microangiographic method have been described elsewhere (Umetani et al., 2007). Briefly, after anesthesia with pentobarbital sodium (50 mg/kg i.p.), bilateral femoral arteries were cannulated for the recording of mean arterial blood pressure and for taking arterial blood samples and inducing hemorrhagic stepwise hypotension. After the ECA had been cannulated to inject the contrast medium, the rats were placed in the supine position in a stereotaxic frame. Rats were intubated and the temperature monitored and controlled at 36–37 °C with a thermo-controlled heating pad. Artificial ventilation of air was maintained by a ventilator at a rate of 60–70 respirations/min. To visualize the perforating and cortical vessels of the hemisphere in a single-view 9.5 mm×9.5 mm frame, rats were tilted at 70° angles to the X-ray beamline and 7° angles in the vertical direction.

After preparation of the animals, the contrast tube inserted in the ECA was connected to an automated injector programmed to deliver 0.3 ml of non-ionic contrast media in 0.6 s. The first angiogram was then obtained to estimate the basal tone of the vessels and we allowed at least 3 min intervals between angiograms to reestablish physiological blood flow before the next angiographic study. The hypotension required to analyze the vascular reactivity of cerebral vessels was achieved by inducing arterial bleeding. The mean arterial blood pressure (MABP) of each animal was reduced in steps of 20 mm Hg at a rate of −0.22 mm Hg/s, and 4–5 successive angiograms were obtained. Before each angiogram, steady-state level of blood pressure was confirmed, which was defined as variance in blood pressure within 10% of MABP. At an MABP below 40 mm Hg, fragmentation of flow in the vessels under observation occurred frequently and made diameter measurement unreliable. We therefore avoided reducing the blood pressure to less than 40 mm Hg. Blood samples were obtained immediately after the first baseline angiography for the measurement of arterial gas tension, pH, and glucose concentration.

The images were stored digitally, and to generate the subtraction images, 10 original images were added to and subtracted from the pre-infusion image. Sequential images were obtained with an input field of 9.5 mm×9.5 mm view and pixel size of 9.5 μm per side. Quantitative measurement of vessel diameter changes by less than the pixel size was achieved by calculating the vessel diameters semi-automatically on the digital image with Image Pro Plus Ver. 5.0 (Media Cybernetics, Inc., Silver Spring, MD) combined with a program especially developed for this study (Oizumi et al., 2006). With this semi-automatic measurement, vessel intensity profiles orthogonal to a smoothed trace in the vessel are picked up, and the vessel diameter is estimated as the width of the intensity profiles.

Table 1
Baseline diameters of perforating and cortical arteries

Range of vascular diameter (μm)	Perforating arteries (μm)*	Cortical arteries (μm)*	P value
20–40	32.7±4.6	35.9±4.3	0.17
40–60	48.1±5.7	48.2±4.8	0.83
60–80	68.4±3.5	70.7±5.0	0.15
80–100	–	86.8±5.1	–
100–120	–	107.0±6.0	–
20–80	51.0±9.8	50.3±12.6	0.79

* Data were presented as average±SD.

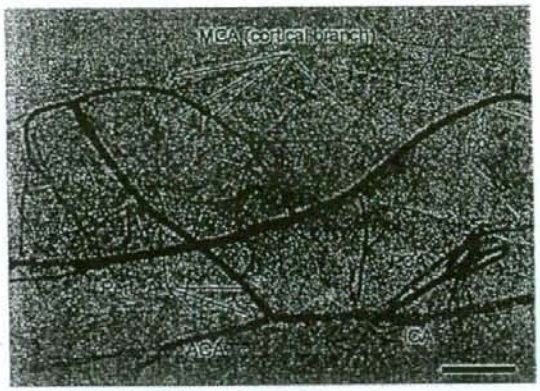

Fig. 1. A representative angiographic view of the cerebral vessels in hemisphere. ICA, internal carotid artery; ACA, anterior cerebral artery; MCA, middle cerebral artery; PCA, and posterior cerebral artery; Perf A, perforating arteries; ppA, pterygopalatine artery.

Statistical analysis

Data are shown as average±SD. Non-paired t-test and two-way analysis of variance (ANOVA) were used for comparisons among the groups. Post-hoc comparisons between mean values were made with the Dunnet test. P values <0.05 were accepted as statistically significant.

Results

Mean arterial blood pressure at baseline was 110.5±2.9 mm Hg, while arterial pH, PaO_2 and $PaCO_2$ were 7.41±0.03, 92±5 mm Hg, and 36±9 mm Hg, respectively. During hypotension, pH was 7.37±0.08, PaO_2 94±5 mm Hg, and $PaCO_2$ 34±5 mm Hg. Perforating arteries 20–80 μm in diameter and cortical vessels 20–120 μm in diameter were measured. We grouped cerebral vessels into five caliber sizes (20–40 μm, 40–60 μm, 60–80 μm, 80–100 μm, and 100–120 μm), because the changes in arterial caliber in response to changes in arterial blood pressure are size-dependent (Kontos et al., 1978). The mean vessel diameters of the groups are shown in Table 1, demonstrating that there were no significant differences in vascular caliber between perforating and cortical arteries.

A representative microangiographic view of the whole hemisphere is shown in Fig. 1. In this image we can clearly see the internal carotid artery, anterior cerebral artery, middle cerebral artery (MCA), posterior cerebral artery and perforating arteries. Some perforating arteries can be seen to emerge from the first portion of the MCA while the second and third ramification of the MCA could also be visualized in a single angiographic view.

Fig. 2A shows steady-state responses of caliber increment to stepwise hypotension of perforating and cortical arteries 20–80 μm in diameter. Baseline diameters of these arteries were not significantly different (Table 1), but perforating arteries exhibited significant vasodilatation at a blood pressure below 80–99 mm Hg and a progressive increase in vascular calibers in response to stepwise hypotension, while cortical arteries showed a gradual and smaller vasodilatation. Significant dilatation was observed in the cortical branches of MCA at a blood pressure below 60–79 mm Hg, so that the vascular response pattern of perforating and cortical arteries was also significantly different (ANOVA).

Because autoregulatory distensibility of cerebral vessels largely depends on the vascular size (Kontos et al., 1978), maximal vasodilatation at a blood pressure of 40–59 mmHg for each vessel size is shown in Fig. 2B. In response to induced hypotension, both perforating

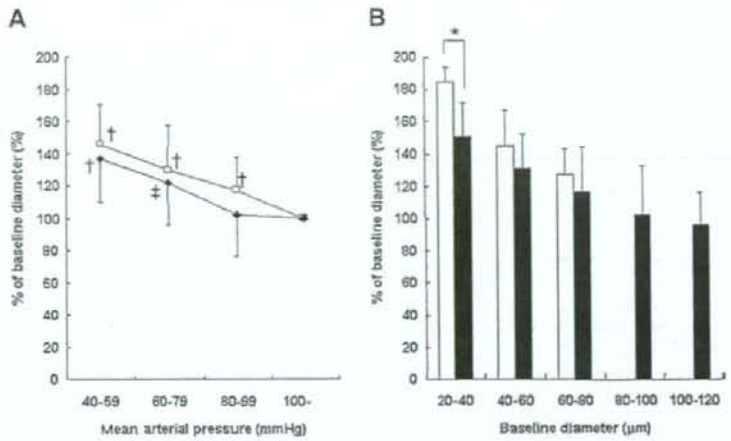

Fig. 2. (A) Steady-state responses of perforating and cortical arteries 20–80 μm in diameter to stepwise hypotension. Perforating arteries (white squares) exhibited significant vasodilatation at a blood pressure below 80–99 mm Hg and a progressive increase in vascular calibers in response to stepwise hypotension. Cortical vessels (black diamonds) showed a gradual and smaller vasodilatation. † and ‡ indicate $P<0.0001$ and $P<0.001$ vs. normal blood pressure, respectively (ANOVA). (B) Maximal vasodilatation of perforating and pial arteries in response to induced hypotension (40–59 mm Hg). Both perforating (white bar) and cortical (black bar) arteries showed significant dilatation. Perforating arteries 20–40 μm in caliber showed a 185.0% increase in dilatation, while cortical arteries of the same diameter showed a 152.7% increase compared with baseline diameter. Asterisks denote $P=0.003$ vs. perforating arteries.

and cortical arteries clearly showed vasodilatation and perforating arteries 20–40 μm in caliber showed 185.0% dilatation compared with the baseline diameter. Larger perforating vessels also dilated significantly, but the percentage increase in diameter in response to hypotension was greater in the smaller than in the larger vessels. On the other hand, cortical arteries showed less vascular dilatation than perforating arteries, with maximal dilatation of cortical vessels 20–40 μm in diameter of 152.7% ($P=0.003$ vs. perforating vessels).

Discussion

In this study, we modified the microangiographic technique by tilting the rat brain to the X-ray beamline so as to focus on autoregulatory response to hypotension of perforating vessels in comparison with that of cortical arteries. Our results clearly indicated that both perforating and cortical arteries dilated in response to induced hypotension and that regulation of distensibility of perforating vessels was more sensitive and pronounced than that of cortical arteries. To the best of our knowledge, this is the first in vivo evidence of a functional difference between perforating and pial arteries, which strongly supports the notion that effective autoregulatory responses of perforating arteries are crucial for maintaining microcirculation of deep brain structures.

Barzo et al. (1993) reported that the functioning of autoregulation in the deep gray matter is strongly influenced by the rate of change in systemic arterial blood pressure. They found that CBF remained at baseline values if hypotension was produced at a rate slower than −0.4 mm Hg/s. Otherwise, the reduction in CBF was similar to that in MABP. In our experiments, stepwise hypotension was induced slowly (−0.22 mm Hg/s) and the steady-state level of blood pressure was confirmed before each angiogram. Thus, it seems likely that autoregulatory responses of cerebral vessels were functioning at each step of hypotension induction.

Baumbach and Heistad (1985) pointed out the regional heterogeneity of cerebral vascular autoregulation, and Mueller, Heistad and Marcus (1977) showed that autoregulation of blood flow is more effective in the brain stem than in the cerebrum. In the pial arterioles, progressive vasodilatation has been demonstrated at a blood pressure below 80 mm Hg (Kontos et al., 1978), which agrees with our results. Our study also found that perforating arteries showed more pronounced and sensitive autoregulatory responses to changes in blood pressure. Three possibilities have to be considered to explain the regional differences in autoregulatory vascular responses: difference in the anatomical structure of vessels, difference in changes in intravascular pressure, and difference in regulation of autoregulatory vasodilatation.

Anatomical studies of human brain have revealed that pial arteries on the cortical surface are generally equipped with two to three muscle layers, whereas penetrating arteries have only one to two smooth muscle cells per circumference (Lamport and Baez, 1962; Edvinsson and Krause, 2001). The same structural elements are noted in rat cerebral vessels, but with smaller dimensions (Edvinsson and Krause, 2001). These structural differences of vessels suggest the wall of pial arteries is less elastic, while another possible implication is that the change of intravascular pressure in pial arteries is smaller. Autoregulatory changes in the caliber of the upstream larger vessels are sufficient to compensate for changes in arterial blood pressure and therefore pressure changes in pial arteries are smaller than the associated changes in mean arterial blood pressure (Lamport and Baez, 1962; Stromberg and Fox, 1972). In contrast, perforating arteries are more proximal and may more strongly reflect the changes in systemic blood pressure. Finally, mechanisms that mediate autoregulation of cerebral blood vessels may include myogenic responses, metabolic factors, neural mechanism and activation of potassium channels (Faraci and Heistad, 1998). Myogenic regulation, neural mechanism and metabolic influences surrounding perforating and cortical vessels may be different, but the precise mechanism of autoregulatory responses in perforating vessels remains unknown.

Because perforating arteries do not have any compensatory mechanism other than autoregulatory vasodilatation, it seems likely that the sensitive and pronounced response of these vessels is mainly responsible for sustaining microcirculation of the deep brain regions during hypotension, so that deterioration of this response could cause serious brain damage. Cerebral small-vessel disease is pathologically characterized by multiple lacunae and widespread white matter lesions, with hypertension as a major risk factor (Yanagihara, 2002, Khan et al., 2007). Stroke-prone spontaneously hypertensive rats (SHR-SP) provide an excellent model for small-vessel disease, because

these rats show chronic hypertension, structural alterations of small cerebral arteries, reduction in cerebral blood flow and white matter lesions (Yamori and Horie, 1977; Lin et al., 2001; Fujita et al., 2008). We recently also investigated autoregulatory responses of the perforating arteries in SHR-SP (Morishita et al., 2006). Our microangiographic studies revealed that perforating arteries of SHR-SP are already dilated under normal blood pressure and therefore lose their distensibility in response to induced hypotension. Pathological alterations of perforating arteries observed in SHR-SP may result in a reduced compensatory response to an increase in blood flow during hypotension. This implies that impaired vascular responses of perforating arteries deserve to be recognized as partly responsible for the pathogenesis of cerebral small-vessel disease.

Following limitations are considered. 1) Although changes of vascular caliber were consistently measured in this study, changes in local CBF during stepwise hypotension were not determined. Combined observation of CBF by means of laser-Doppler flowmetry (Barzo et al., 1993) would help to reveal the microcirculation of deep brain regions more precisely. 2) Angiographic analysis of the present study was performed under the anesthesia with pentobarbital sodium. Effects of barbiturates on the cerebral vessels have not been evaluated. However, any differential effects of pentobarbital on perforating and cortical arterioles have not been demonstrated (Hendrich et al., 2001).

On the other hand, angiographic imaging of the perforating arteries in comparison with cortical arterioles has several impacts for the medical community. This study facilitates the investigation of not only the microcirculation in the deep brain region, but also the pathogenesis of the cerebral small-vessel disease in atherosclerotic conditions, such as ageing, hypertension and diabetes. Further steps of research can be conducted to find the molecular basis of impaired cerebrovascular reactivity using the rodent models for neurological disorders (Kidoguchi et al., 2006).

Acknowledgments

This work was supported by a Research Grant from the Novartis Foundation for Gerontological Research and a Grant-in-Aid for Scientific Research (17500473) from the Japan Society for the Promotion of Science (T.S.). Synchrotron radiation experiments were performed at the SPring-8 BL28B2 beamline with the approval of the Japan Synchrotron Radiation Research Institute (Acceptance Nos. 2002A0079-NL2-np, 2002B0312-NL2-np, and 2004A0313-NL3-np).

References

Barzo, P., Bari, F., Tamas, D., Gabor, J., Mihaly, B., 1993. Significance of the rate of systemic change in blood pressure on the short-term autoregulatory response in normotensive and spontaneously hypertensive rats. Neurosurgery 32, 611–618.
Baumbach, G., Heistad, D., 1985. Regional, segmental and temporal heterogeneity of cerebral vascular autoregulation. Ann. Biomed. Engi. 13, 303–310.
Edvinsson, L., Krause, D., 2001. The blood vessel wall. Endothelial and smooth muscle cells. In: Edvinsson, L., Krause, D. (Eds.), Cerebral Blood Flow and Metabolism, 2nd Edition. Lippincott Williams & Wilkins, pp. 30–41.
Faraci, F.M., Heistad, D.D., 1998. Regulation of the cerebral circulation: role of endothelium and potassium channels. Physiol. Rev. 78, 53–97.
Fujita, Y., Lin, J.X., Takahashi, R., Tomimoto, H., 2008. Cilostazol alleviates cerebral small-vessel pathology and white-matter lesions in stroke-prone spontaneously hypertensive rats. Brain Res. [Epub ahead of print].
Hendrich, K., Kochanek, P., Melick, J., Schiding, J., Statler, K., Williams, D., Marion, D., Ho, C., 2001. Cerebral perfusion during anesthesia with fentanyl, isoflurane, or pentobarbital in normal rats studied by arterial spin-labeled MRI. Magn. Reson. Med. 46, 202–206.
Jorgensen, H., Nakayama, H., Raaschou, H.O., Olsen, T.S., 1994. Stroke in patients with diabetes. The Copenhagen Stroke Study. Stroke 25, 1977–1984.
Khan, U., Porteous, L., Hassan, A., Markus, H.S., 2007. Risk factor profile of cerebral small vessel disease and its subtypes. J. Neurol. Neurosurg. Psychiatry 78, 702–706.
Kidoguchi, K., Tamaki, M., Mizobe, T., Koyama, J., Kondoh, T., Kohmura, E., Sakurai, T., Yokono, K., Umetani, K., 2006. In vivo X-ray angiography in the mouse brain using synchrotron radiation. Stroke 37, 1856–1861.
Kontos, H.A., Wei, E.P., Navari, R.M., Levasseur, J.E., Rosenblum, W.I., Patterson Jr., J.L., 1978. Responses of cerebral arteries and arterioles to acute hypotension and hypertension. Am. J. Physiol. 234, H371–H383.
Lamport, H., Baez, S., 1962. Physical properties of small arterial vessels. Physiol. Rev. Suppl. 5, 328–352.
Lin, J.X., Tomimoto, H., Akiguchi, I., Wakita, H., Shibasaki, H., Horie, R., 2001. White matter lesions and alteration of vascular cell composition in the brain of spontaneously hypertensive rats. Neuroreport 12, 1835–1839.
Molina, C., Sabin, J.A., Montaner, J., Rovira, A., Abilleira, S., Codina, A., 1999. Impaired cerebrovascular reactivity as a risk marker for first-ever lacunar infarction: a case-control study. Stroke 30, 2296–2301.
Morishita, A., Kondoh, T., Sakurai, T., Ikeda, M., Bhattacharjee, A.K., Nakajima, S., Kohmura, E., Yokono, K., Umetani, K., 2006. Quantification of distension in rat cerebral perforating arteries. Neuroreport 17, 1549–1553.
Mueller, S.M., Heistad, D.D., Marcus, M.L., 1977. Total and regional cerebral blood flow during hypotension, hypertension, and hypocapnia. Effect of sympathetic denervation in dogs. Circ. Res. 41, 350–356.
Oizumi, X.S., Akisaki, T., Kouta, Y., Song, X.Z., Takata, T., Kondoh, T., Umetani, K., Hirano, M., Yamasaki, K., Kohmura, E., Yokono, K., Sakurai, T., 2006. Impaired response of perforating arteries to hypercapnia in chronic hyperglycemia. Kobe J. Med. Sci. 52 (1–2), 27–35.
Stromberg, D.D., Fox, J.R., 1972. Pressures in the pial arterial microcirculation of the cat during changes in systemic arterial blood pressure. Circ. Res. 31, 229–239.
Umetani, K., Kidoguchi, K., Morishita, A., Oizumi, X.S., Tamaki, M., Yamashita, T., Sakurai, T., Kondoh, T., 2007. In vitro cerebral artery microangiography in rat and mouse using synchrotron radiation imaging system. Proc. 29th Annual Int. Conf. of the IEEE Engineering in Medicine and Biology Society, pp. 3926–3929.
Yamori, Y., Horie, R., 1977. Developmental course of hypertension and regional cerebral blood flow in stroke-prone spontaneously hypertensive rats. Stroke 8, 456–461.
Yanagihara, T., 2002. Vascular dementia in Japan. Ann. N. Y. Acad. Sci. 977, 24–28.

ELSEVIER

Neurobiology of Aging 29 (2008) 1022–1026

NEUROBIOLOGY OF AGING

www.elsevier.com/locate/neuaging

Factors associated with lower Mini Mental State Examination scores in elderly Japanese diabetes mellitus patients

Hiroyuki Umegaki [a,*], Satoshi Iimuro [b], Tetsuji Kaneko [c], Atsushi Araki [d], Takashi Sakurai [e], Yasuo Ohashi [c], Akihisa Iguchi [a], Hideki Ito [f]

[a] *Department of Geriatrics, Nagoya University Graduate School of Medicine, 65 Tsuruma-Cho, Showa-Ku, Nagoya, Aichi 466-8550, Japan*
[b] *Department of Cardiovascular Medicine, Graduate School of Medicine, University of Tokyo, Tokyo, Japan*
[c] *Department of Biostatistics, School of Health Sciences and Nursing, University of Tokyo, Tokyo, Japan*
[d] *Department of Endocrinological Medicine, Tokyo Metropolitan Geriatric Medical Center, Tokyo, Japan*
[e] *Department of Internal and Geriatric Medicine, Kobe University Graduate School of Medicine, Kobe, Japan*
[f] *Tokyo Metropolitan Geriatric Medical Center, Tokyo, Japan*

Received 22 April 2006; received in revised form 8 January 2007; accepted 5 February 2007
Available online 16 April 2007

Abstract

Cognitive impairment in elderly diabetic patients has generated considerable interest recently; however, the mechanism of the impairment remains to be elucidated. In the current study, factors associated with cognitive dysfunction in old diabetic patients were explored. A Mini Mental State Examination (MMSE) was performed on 907 of 1173 registered elderly Japanese diabetic subjects. To characterize the clinical features of diabetes, we examined indices of glycemic control, lipid metabolism, blood pressure and complications. Single regression analysis adjusted for age showed that shorter height, higher GDS 15 scores, lower serum albumin, history of cerebrovascular disease, the existence of diabetic nephropathy, no smoking habit, no drinking habit, and no occupation were associated with lower MMSE scores. Multiple regression analysis demonstrated that age (odds ratio (OR) = 1.079; 95% confidence interval (CI) = 1.011–1.150), GDS 15 scores (OR = 1.139; 95% CI = 1.045–1.243), serum albumin (OR = 0.336; 95% CI = 0.174–0.745), and history of cerebrovascular disease (OR = 3.011; 95% CI = 1.578–5.748) were the variables significantly associated with having lower MMSE scores.

Keywords: Cognition; Dementia; Serum albumin; Cerebrovascular accident; Depression

1. Introduction

The prevalence and incidence of diabetes mellitus (DM) are increasing at all ages, including older populations, and approximately 15% of the elderly population in Japan is affected. Multiple metabolic abnormalities in DM induce systemic complications, which may include microangiopathic complications (neuropathy, retinopathy, nephropathy) and macroangiopathic atherosclerosis (stroke and ischemic heart disease). Several studies have shown that elderly diabetics have impaired cognition compared to age-matched non-diabetics, as well as a higher risk of dementia (Cukierman et al., 2005; Mogi et al., 2004; Strachen et al., 1997). Because the increase in the number of elderly people with cognitive impairment or dementia creates significant medical, social and economic burdens, cognitive impairment in older DM subjects has recently sparked considerable interest. It is highly desirable to be able to provide intervention in the case of older DM subjects who are at risk for cognitive decline or dementia in order to preserve cognitive functions; however, the mechanism of DM-associated cognitive decline remains to be elucidated and there is no solid evidence as yet that any treatment for DM is effective in preventing cognitive decline (Areosa Sastre and Grimley Evans, 2007). In order to establish an effective way of treating or preventing

* Corresponding author. Tel.: +81 52 744 2365; fax: +81 52 744 2371.
E-mail address: umegaki@med.nagoya-u.ac.jp (H. Umegaki).

0197-4580/$ – see front matter © 2007 Elsevier Inc. All rights reserved.
doi:10.1016/j.neurobiolaging.2007.02.004